Kinetics of RNA Replication: Plus–Minus Asymmetry and Double-Strand Formation†

Christof K. Biebricher, Manfred Eigen, and William C. Gardiner, Jr.*

ABSTRACT: The effects of kinetic plus–minus asymmetry and formation of inactive double strands on the self-replication of single-stranded RNA were investigated by analytical and computer simulation methods. It was found that extensions of the analysis developed previously for more restricted models lead to simple formulations that can be used for interpretation of experiments. Relaxation to linear growth or to steady-state conditions for double-strand formation was found to depend upon initial conditions but to be essentially complete for typical laboratory situations. Experimental data confirmed that in the linear growth phase the total nucleotide incorporation rate is about equal in the complementary strands; mostly double strand is formed. However, the enzyme is usually not shared equally, and some steps proceed at different rates in the two strands. The asymmetry is, however, not found to be dramatic for any of the RNA variants studied so far. It appears that the observed prevalence of kinetically rather symmetric self-replication is due to selection of RNA species with similar rate constants during the exponential growth phase.

Laboratory studies of genetic information transfer based on the self-replication of suitable single-stranded RNA species by the enzyme Qβ replicase have proved to be fruitful in providing insight into the processes of natural selection and evolution at the molecular level (Biebricher, 1983). In an earlier paper (Biebricher et al., 1983), we investigated RNA self-replication by conventional methods of chemical kinetics analysis. It was found that traditional concepts of enzyme catalysis could be adapted for self-replicating systems despite the inherent mechanistic complexities and that under suitable simplifications one can derive compact formulas helpful in describing laboratory observations. To obtain these formulas, it was useful to restrict the analysis to kinetically symmetric cases, i.e., to assume that the rate constants pertaining to plus-strand replication were the same as those pertaining to minus-strand replication. Furthermore, it was assumed that RNA is present only in the catalytically active single-stranded form even though annealing to double strands inactive as template must occur with some rate constant whenever plus and minus strands are present simultaneously and can even be a dominant process for some template strands.

In this paper, we report analytical and computer simulation results for the more general cases in which plus–minus asymmetry and a finite double-strand formation rate are important. It is shown that extension of the methods used previously leads to compact analytical expressions in which the asymmetry and double-strand formation effects can be clearly seen.

Materials and Methods

The mathematical techniques used for this investigation were essentially the same as those for our previous investigation (Biebricher et al., 1983). All computer simulations were done on the Univac 1100/83 of the Gesellschaft für Wissenschaftliche Datenverarbeitung, Göttingen, in single precision using the IMSL version of Gear's algorithm at a tolerance level sufficiently accurate to preserve integration accuracy and matter conservation at $1/10^4$ or better.

Separation of Plus and Minus Strands of the RNA Variants. MDV-1 was separated according to Mills et al. (1978) and MNV-11 by gel electrophoresis of melted strands in 14% acrylamide gels in 0.1 M tris(hydroxymethyl)aminomethane (Tris)–borate buffers (pH 8.3) at 4 °C. For measurement of enzyme-bound RNA, the variants were grown as follows. A mixture containing per milliliter 50 μmol of Tris-HCl (pH 7.5), 10 μmol of $MgCl_2$, 0.5 μmol each of CTP, GTP, UTP, and [α-^{32}P]ATP (sp act. 100 Ci/mol), 100 pmol of Qβ replicase, and 1 pmol of template was incubated at 30 °C for 2 h. The ratio of RNA to enzyme at this time was about 10. Enzyme-bound RNA was isolated by filtration through nitrocellulose filters applied to the separation gels, after which the strands were separated by electrophoresis under the above conditions. Elongation intermediates were not detected.

Results

Reaction Mechanism. Our study is based upon the reaction mechanism shown in Figure 4 of our previous paper (Biebricher et al., 1983) to which the reader is referred for justifications and nomenclature. In addition to the steps shown in the general mechanism before, we now include formation of $I^+:I^-$, double-stranded RNA inactive as template, by the reaction

$$I^+ + I^- \rightarrow I^+:I^-$$

which is assumed not to involve enzyme catalysis and to be irreversible. It was found convenient for developing analytical expressions to consider two alternative simplifications of the general mechanism. In the *consecutive release* model (Figure 1a), it is assumed that replica release occurs in step 1 and template release in step 2. The RNA-bound enzymes $E_c^{\pm}$ are then composed nearly entirely of the last replication intermediates ${}_nIE^{\pm}$. This model is suggested by the experimental results of Dobkin et al. (1979) and Biebricher et al. (1981) for short RNA variants. In the *concurrent release* model (Figure 1b), it is assumed that replica release is formally concurrent with enzyme and template release. This model would be appropriate for a replication process whose rate is limited by the elongation steps. Here, templates $I^{\pm}$ bind to the replicase E to form replication intermediates $E_c^{\pm}$ which dissociate in the second step to release template and replica,

† From the Max-Planck-Institut für Biophysikalische Chemie, D-3400 Göttingen, Federal Republic of Germany (C.K.B. and M.E.), and the Department of Chemistry, University of Texas, Austin, Texas 78712 (W.C.G.). *Received November 7, 1983.* This research was carried out under the auspices of the Max-Planck-Gesellschaft. Additional support from the Alexander von Humboldt, Fritz Thyssen, and Robert A. Welch Foundations is also acknowledged.

0006-2960/84/0423-3186$01.50/0

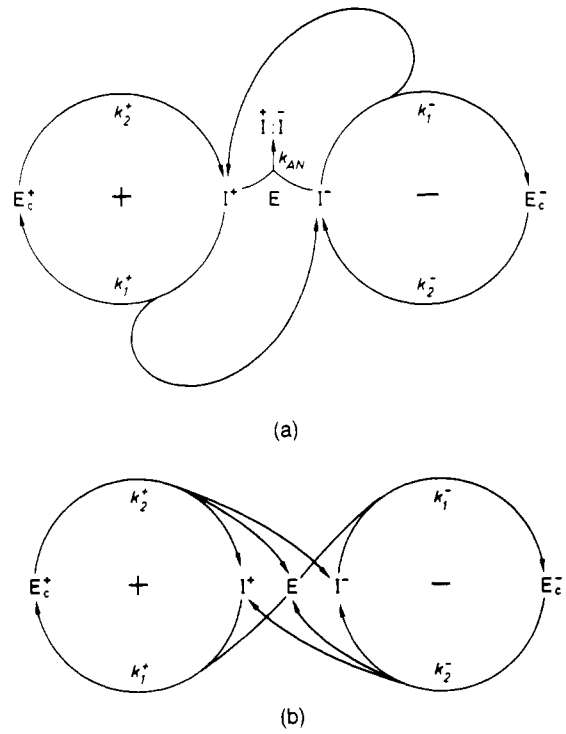

FIGURE 1: Simplified reaction mechanisms: (a) consecutive release, replica release occurs in step 1; (b) concurrent release, replica release occurs in step 2. E is free enzyme; I^+ and I^- are free RNA strands; I^+:I^- is double-stranded RNA; E_c^+ and E_c^- are enzyme–template complexes. Comparison with the full mechanism (Biebricher et al., 1983, Figure 4) shows that the steps indicated here as 1 and 2 are schematic only and correspond to groups of elementary reactions.

I^+ and I^-, and enzyme E. In this case, $E_c^{\pm}$ contains mainly the elongation intermediates denoted in the full mechanism as ${}_jIEP_j^{\pm}$. For each cycle, second-order rate constants k_1^+ and k_1^- are assigned to the first step and first-order rate constants k_2^+ and k_2^- to the second step. While the rate equations (Appendix I) are different for the two models, the final analytical expressions are shown to be identical in form for some cases.

Since these simplified mechanisms combine the template binding, initiation, and elongation processes into a single step, a dependence upon enzyme concentration appears that really pertains only for low enzyme concentration, where elongation is rapid compared to template binding. For higher enzyme concentrations, saturation occurs, and the rate of step 1 is independent of enzyme concentration, representing instead the overall rate of the initiation and elongation processes. Experimentally, it was indeed found (Biebricher et al., 1981b) that under enzyme saturation conditions the growth rate is independent of enzyme concentration until the RNA concentration exceeds the enzyme concentration.

It is convenient to develop the analytical expressions independently for three cases: the linear growth situation that pertains when enzyme is saturated with template; the steady-state situation in which all concentrations remain constant except for the growing concentration of double-stranded RNA; and the exponential growth situation prevailing when the enzyme concentration is much larger than the RNA concentration.

Linear Growth. When the enzyme is saturated with template and a steady state is reached for the replication intermediates, the total enzyme concentration $[E_0]$ is divided into $[E_c^+]$ and $[E_c^-]$ in a ratio that does not change in time. We assume that the free enzyme concentration [E] is so much smaller than the concentrations of the replication complexes that it can be neglected. Substitution of the steady-state equations (derivatives of $[E_c^+]$ and $[E_c^-]$ set equal to zero) into the rate equations for I^+ and I^- (Appendix I) reduces them for both concurrent and consecutive release cases to

$$d[I^+]/dt = k_2^-[E_c^-] \qquad d[I^-]/dt = k_2^+[E_c^+]$$

In the steady state, the ratio $[I^+]/[I^-]$ is maintained at the constant value $[I^+]/[I^-] = (k_1^-/k_1^+)^{1/2}$. This can be seen by substituting the preceding rate equations for I^+ and I^- and the steady-state equations for $[E_c^+]$ and $[E_c^-]$ into the derivative of the quotient $([I^+]/[I^-])$ to get

$$d([I^+]/[I^-])/dt = [E][k_1^- - k_1^+([I^+]/[I^-])^2]$$

which shows that any deviations from the steady-state $[I^+]/[I^-]$ ratio are counteracted by opposing reaction.

Combining the equations for $[E_c^+]$, $[E_c^-]$, and $[I^+]/[I^-]$ then permits derivation of the expressions in Appendix II. Numerical integration of the original kinetic equations for a variety of initial conditions and rate constant sets showed that relaxation into the steady-state concentration ratios was usually complete to 1% within 2τ and that better than $1/10^3$ accuracy is attained within 10τ in all cases.

The procedure used for generating the Appendix II expressions can be generalized for the complete mechanism of stepwise polymerization introduced in our previous paper for the palindromic case of the symmetric mechanism. At the steady-state values of $[E_c^+]$ and $[E_c^-]$, the previous expressions for the palindromic mechanisms [Figure 5 and Table II of Biebricher et al. (1983)] apply with substitution of $[E_c^+]$ and $[E_c^-]$ for $[E_0]$ in the rate equations

$$\frac{d[I^+]}{dt} = v^- \frac{[E_c^-]}{[E_0]} \qquad \frac{d[I^-]}{dt} = v^+ \frac{[E_c^+]}{[E_0]}$$

While the overall rate v in the palindromic cycle is proportional to the constant total enzyme concentration $[E_0]$, v^+ and v^- in the asymmetric cycle, also proportional to $[E_0]$, are multiplied by the fractions of the total enzyme bound in the replication complexes with minus- and plus-strand templates, respectively, to give the production rates of I^+ and I^-. Otherwise, the enzyme is distributed among the intermediate complexes as in the palindromic cycle.

The asymmetric steady state is characterized by the following three conditions. (1) The *relative* changes of $[I^+]$ and $[I^-]$ are balanced:

$$d \ln [I^+]/dt = d \ln [I^-]/dt$$

(2) For each replication intermediate in the cycle there is a balance between formation and destruction rates, giving, for instance, for the concentration of the active enzyme–template complex the expression

$$[{}_1I^+E] = \frac{k_{A3'}^+[I^+][E]}{k_{D5'}^+ + k^*{}_{12}^+[S_0]}$$

(3) The production rates of I^+ and I^- are equal to the fluxes through the complementary cycles, which are the same from step to step at the steady state. Therefore, the production rates can be related to the primary (or any other) steps as

$$v^+([E_c^+]/[E_0]) = k^*{}_{12}^+[S_0][{}_1I^+E]$$

Combining these conditions with $[E_0] = [E_c^+] + [E_c^-]$ yields generalized steady-state expressions, which are summarized in Appendix III.

Plus–minus asymmetry therefore does not change the general nature of the linear growth phase found for the palindromic cycle. It is characterized by constant rates for each

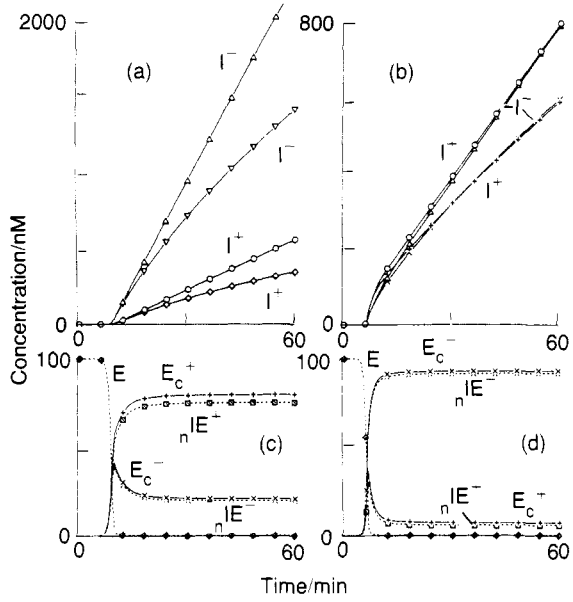

FIGURE 2: Computer simulations showing concentration vs. time profiles for the linear growth phase. Standard k values (Biebricher et al., 1983) were used, except that $k_{PI} = 0$ for (b) and (d), and (a and c) $k_{A3'}{}^+ = 4 \times 10^7$ M^{-1} s^{-1} and $k_{A3'}{}^- = 0.25 \times 10^7$ M^{-1} s^{-1} and (b and d) $k_{D5'}{}^+ = 0.04$ s^{-1} and $k_{D5'}{}^- = 0.0025$ s^{-1}. The lower lines in (a) and (b) show the deviation from linearity caused by product inhibition.

cycle, proportionality to $[E_c]$, and contribution of all rate terms to the overall rate v. The expressions in Appendix III show that plus–minus asymmetry in the production rates is introduced solely by asymmetry in the template binding rate constants k^*_{TB}. If they are equal for both cycles, then I^+ and I^- are produced at the same rate, which is half of the harmonic mean of v^+ and v^- (Figure 2). In the exponential growth phase, by contrast, it is essentially the geometric mean of the two individual reproduction rates that governs. This is a fundamental difference, because in a harmonic mean the smaller term dominates while in a geometric mean both contribute in a balanced way. It should be noted that k^*_{TB} is approximately equal to the elementary rate constant $k_{A3'}$ if $k_{D3'}$ is very small. This condition seems to be fulfilled in most cases: Nishihara et al. (1983) were able to isolate template–enzyme complexes by sedimentation for many hours. Dissociation of template–enzyme complexes is thus so slow that it can be neglected.

The simple analogy to the expressions derived for the palindromic cycle also shows how one can amend the Appendix III expressions for variations upon the basic mechanism, such as direct 5′–3′ reactivation or phosphorylysis.

These results pertain to a true steady state, and both experiments and computer simulations confirm that the steady state is not fully established for typical conditions used in experiments on Qβ replicase. On the one hand, the transition to steady growth requires gradual attainment of the steady-state concentrations of all intermediates; on the other, product inhibition manifests itself as a gradual slowing of the linear growth rate fairly soon after enzyme saturation is essentially complete. These effects are illustrated in the computer simulations shown in Figure 2. While the computer simulations demonstrate that the linear growth phase is an ideal situation realized in experiments only as an approximation, they also confirm that the analytical expressions given in Appendix II and III are correct descriptions of it.

Formation of Double-Stranded RNA. So far, we have considered only the effects of rate constant asymmetries between complementary plus and minus strands. Making this distinction raises the question of their direct chemical interaction, a question that was also neglected in our earlier study of palindromic self-replication. Significant formation of double-stranded RNA inactive as template is indeed observed for some RNA species that can be self-replicated by Qβ replicase (Biebricher et al., 1982). The simplest way to take this into account is by adding a single nonenzymatic and irreversible bimolecular reaction between I^+ and I^-. We assumed that enzyme-bound RNA does not participate and that double strands do not compete with single strands for free replicase. Experiments in our group showed that double-stranded RNA can bind to replicase but that the resulting complexes are much weaker than those with template RNA and dissociate rapidly [unpublished results; see also Silverman (1973) and Nishihara et al. (1983)].

The degree to which double-strand formation interferes with the replication process depends upon its competition with replication complex formation, or in kinetic terms upon the products $k_{ds}[I^+][I^-]$ and $k_{A3'}{}^+[I^+][E]$ for the plus strand or $k_{ds}[I^+][I^-]$ and $k_{A3'}{}^-[I^-][E]$ for the minus strand. Depending upon the relative magnitudes of k_{ds} and $k_{A3'}$, these products may become comparable at concentrations of free single-stranded RNA below, at, or above the enzyme concentration. Experimentally, it would appear that, for those RNA variants studied so far that do anneal, the rate constants are such that double-strand formation already becomes noticeable in the early linear phase where the total RNA concentration is comparable to the enzyme concentration (Biebricher et al., 1982; see also experimental results described below).

There are two effects of double-strand formation that are of interest. First, it eventually causes the growth of single strands to level off, restricting competition between plus and minus strands. Nucleotide incorporation continues to proceed linearly, but only the concentration of double-stranded RNA increases. Second, template destruction may have crucial influence upon selection. In order to assess these effects, it is again useful to consider a steady-state situation, here the one that arises when template production by self-replication is balanced by template destruction by double-strand formation.

The analysis of the consecutive release model (Figure 1a) for the steady state caused by double-strand formation is similar to that used above for the linear growth steady state. The derivatives of all concentrations are exactly zero except for that of the double-stranded RNA, whose growth is the only measure of the production rate of the self-replicating system. In contrast to the linear growth situation in the absence of double-strand formation, we cannot neglect the free enzyme concentration, since for large k_{ds} values there may be significant concentrations of free enzyme present.

The important analytical expressions are summarized in Appendix IV. It is seen that an essential difference from the linear growth situation appears in the linear dependences upon α, the ratio of the rate constants for the first step, rather than square root dependences. The steady-state rate of double-strand production becomes linearly dependent upon $[E_0]$ (cf. the proportionality to $[E]^2$) but does not depend upon k_{ds} in the limit of enzyme saturation with template; if this saturation is not reached, all rate constants are involved in determining the steady-state concentrations and production rate. Computer simulations for the Figure 1a mechanism confirmed that the Appendix IV equations become valid more rapidly than those for the linear growth steady state over all reasonable sets of rate constants. Figure 3 shows computer simulations illustrating the establishment of the double strand induced steady

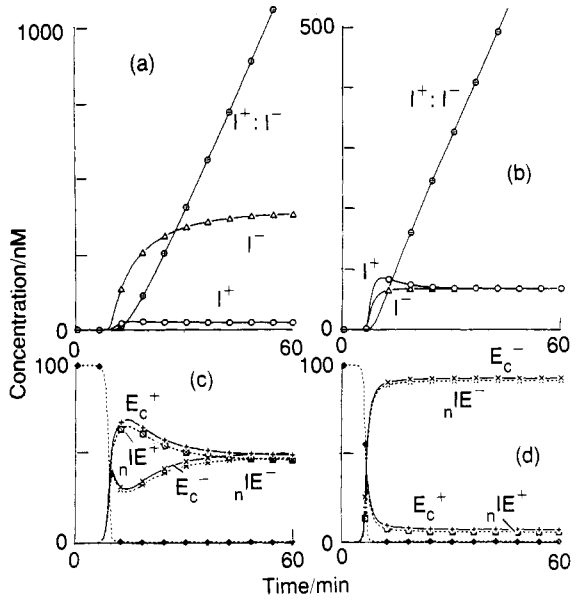

FIGURE 3: Computer simulations showing concentration vs. time profiles for the transition to steady-state double-strand formation. k values as in Figure 2 except $k_{ds} = 5 \times 10^4$ M^{-1} s^{-1}.

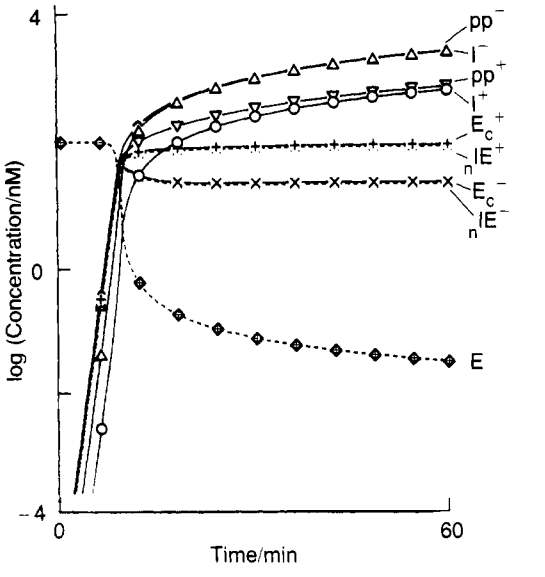

FIGURE 4: Computer simulations showing transition from exponential into linear growth phase. k values are as in Figure 2a. pp^+ and pp^- are pyrophosphate produced in plus and minus replication cycles; $_nIE^+$ and $_nIE^+$ are 5′-bound enzyme–template complexes. Other symbols are as in Figure 1.

state for the full multistep mechanism.

Exponential Growth. The typical feature of this phase is exponential growth of all concentrations with a common rate constant κ (Figure 4.) As in the palindromic case, a rigorous analytical treatment is so involved that explicit expressions can be obtained only for certain limiting cases. These limiting cases, however, are very useful in providing understanding of exponential self-replicative growth. We use the same techniques here for the asymmetric tandem plus–minus self-replication process as were used before for the palindromic case. The limiting cases are as follows: (1) one-step self-replication, in which the rate-limiting step occurs prior to or simultaneously with replica release [this would be given by the consecutive release model (Figure 1a) if step 1 is rate limiting or the concurrent release model (Figure 1b) whichever step is rate limiting]; (2) two-step self-replication, in which the rate-limiting step occurs after replica release, as for slow 5′–3′ reactivation of the enzyme–template complex [we represent this as the consecutive release model (Figure 1a) with step 2 rate limiting]; (3) multistep self-replication, in which no single step is rate limiting, e.g., in which the residence times at all steps of the replication process are equal.

(1) One-Step Self-Replication. Consider the concurrent release model (Figure 1b) where the rate-limiting step occurs either before or simultaneously with replica release. The two ways for the rate-limiting step to occur are formally distinct: it may be associated either with the initial second-order step of template binding or with one of the subsequent steps (initiation, elongation, or replica and template release) that are combined as step 2 of the concurrent release model. As long as the total enzyme concentration is much larger than the RNA concentration, the free enzyme concentration [E] is essentially equal to the constant total enzyme concentration $[E_0]$ for the entire exponential growth phase. The initial second-order step involving free template and free enzyme then reduces to a quasi-first-order step. Appendix V shows the derivation procedure for obtaining analytical expressions for the exponential growth constant κ. The essential conclusion is that whether the first or the second step is rate limiting, the growth constant is given by the geometric mean of the rate constants for the rate-limiting step (Eigen, 1971):

$$k_1^{\pm}[E_0] \ll k_2^{\pm} \qquad \kappa = (k_1^+ k_1^-)^{1/2}[E_0]$$

$$k_1^{\pm}[E_0] \gg k_2^{\pm} \qquad \kappa = (k_2^+ k_2^-)^{1/2}$$

Steady exponential growth follows an induction period of the same magnitude as $1/\kappa$. The ratio of the total RNA concentrations of both strands then remains constant, being inversely proportional to the square root of the ratio of the rate constants for the rate-limiting (slow) step (cf. Appendix VI). The less efficient template thus has a larger concentration than the more efficient one, as observed in other contexts for cooperative populations. In these equations one can see why this has been called one-step self-replication, for in the final equations only one of the two steps finally determines the rate.

(2) Two-Step Self-Replication. Consider next the consecutive release model (Figure 1a). Realistically, step 2 has to be related somehow to reactivation of the 5′-bound template and rebinding at the 3′-end. The solutions (Appendix V) for the limiting cases are as follows. For step 1 rate limiting

$$k_1^{\pm}[E_0] \ll k_2^{\pm} \qquad \kappa = (k_1^+ k_1^-)^{1/2}[E_0]$$

For step 2 rate limiting

$$k_1^{\pm}[E_0] \gg k_2^{\pm} \qquad \kappa = \left[\frac{k_1^+ k_1^-[E_0](k_2^+ + k_2^-)}{k_1^+ + k_1^-}\right]^{1/2}$$

The geometric mean arising when step 1 is rate limiting is a confirmation of the first result obtained above, since the rate-limiting step again occurs before or simultaneously with template release, and we have the third case of one-step self-replication.

The other limiting case, which proves to be the physically meaningful one, yields a different result. It can be understood by recalling that for the palindromic cycle in the $k_1[E_0] \gg k_2$ limit, the whole nature of the autocatalytic amplification process changes. For k_2 extremely small, new template is still formed continuously, but the 5′-bound template stays inactive. Hence, in this limit the production of new template does not lead to an increase of template concentration. As long as k_2 is not zero, the exponential growth constant of the palindromic cycle is the geometric mean $(k_1[E_0]k_2)^{1/2}$ (Biebricher et al., 1983). While this essential property is retained in the asymmetric mechanism, geometric averaging of the growth rates

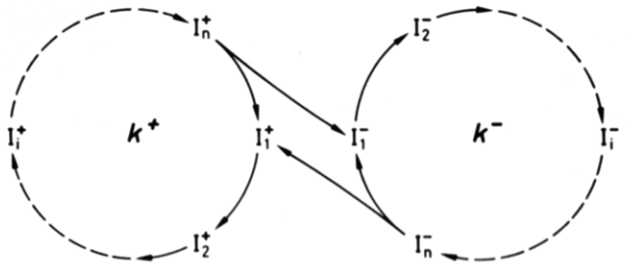

FIGURE 5: Multistep replication mechanism. Since the enzyme concentration is large and constant, $[E] = [E_0]$ can be combined with $k_{A3'}$ to the quasi-first-order rate constant k_1^+. All rate constants are set equal to k^+ or k^-, respectively, in both cycles.

for plus and minus strands does not arise. The growth constant for the case $k_1^{\pm}[E_0] \gg k_2^{\pm}$ is clearly different from geometric averaging of all four k's. The nongeometric average does reduce to the palindromic cycle result if equal rate constants pertain to plus and minus cycles. Its form shows that if plus–minus asymmetries do exist, the smaller of the two k_1 values and the larger of the two k_2 values determine the value of κ. Therefore, the geometric mean expression must be fulfilled for the extremes of both rate constants. The nongeometric average and its approach to the geometric mean limits were checked by computer simulations of the Figure 1 mechanism and of the complete mechanism and found to be valid under the conditions used for the derivation. Appendix VI gives formulas for the important ratios in forms that can be evaluated from the appropriate κ values.

(3) Multistep Self-Replication. Our previous analysis of the palindromic cycle showed that considering a multistep replication process provides new insight into the character of a reaction that cannot be reduced to one or a few rate-limiting steps. The corresponding multistep mechanism for separate plus and minus cycles is shown in Figure 5. The limiting case of the rate being limited by many steps is to distribute the residence times uniformly over all n steps of each cycle by setting all rate constants of the plus cycle equal to k^+ and all rate constants of the minus cycle equal to k^-. This provides an extreme counterexample to the one-step case discussed above.

The solution of the kinetic equations proceeds as described previously for the palindromic cycle and is summarized in Appendix VII [see also Figure 6 and the associated text of Biebricher et al. (1983)]. Since the determinental equation has only one sign change, there is only one positive real eigenvalue, namely, the growth constant κ. Our previous analysis suggests that it is the smallest eigenvalue, i.e., the one with the largest time constant. The equations of Appendix VII clearly show that the growth constant is not simply related to the geometric mean $(k^+k^-)^{1/2}$. For comparison, in the limit of large n of the palindromic case, the exponential growth constant (k/n) ln 2 differs from the linear growth constant by the factor ln 2. As long as the asymmetry factor k^+/k^- is not too far from 1, the differences between the geometric mean equivalent to the palindromic case, $(k^+k^-)^{1/2}$ ln $2/n$, and the actual growth constant are small. For factors of 2 and 4, the discrepancies amount to factors of 0.98 and 0.93. For more pronounced asymmetries, however, they are larger: for $k^+/k^- = 100$, the discrepancy is 0.49. Such extreme asymmetry would be quite unrealistic for complementary RNA strands, and therefore, we expect that actual differences from the geometric mean growth constant should be small. Computer simulations confirmed that similar results are found when the complete mechanism is considered for comparable asymmetries.

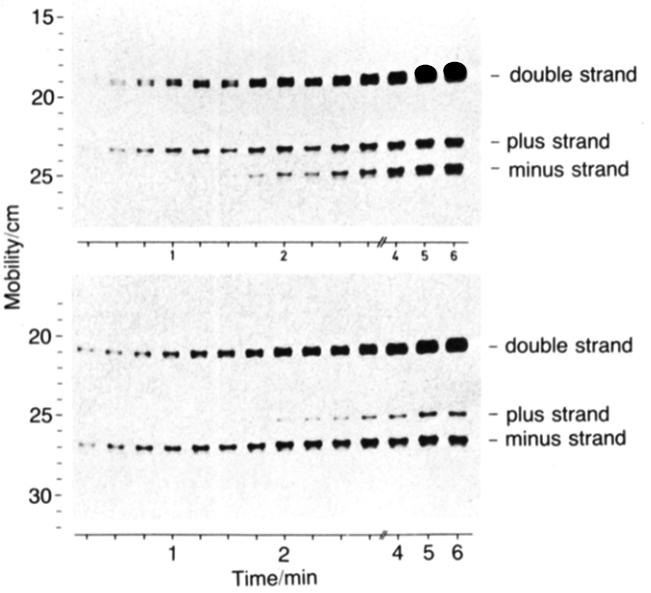

FIGURE 6: Electropherograms of asymmetrically synthetized MNV-11. The reaction mixture contained per milliliter 50 μmol of Tris-HCl (pH 7.5), 10 μmol of $MgCl_2$, 0.5 μmol of CTP, UTP, GTP, and [α-^{32}P]ATP (sp act. 100 Ci/mol), 150 pmol of Qβ replicase, and 175 pmol of template. (Upper part) MNV-11 minus strand template; (lower part) MNV-11 plus strand template. Aliquots of 5 μL were withdrawn at the indicated times, mixed with 5 μL of 0.5% $NaDodSO_4$ and 0.01 M EDTA, and applied to gel in an appropriate separation electrophoresis system.

Experimental Determination of Asymmetry. There is only limited information available about the occurrence of asymmetry in vivo or in vitro. Qβ RNA itself is of course the most notable example: Qβ minus strand is accepted by Qβ replicase alone, while Qβ plus strand also requires the presence of subunit S1 and host factor to be accepted as template (Feix et al., 1968).

The nucleotide composition of variant V-1 (Mills et al., 1966) and the dinucleotide frequencies found in 6S RNA (Prives & Silverman, 1972) suggest asymmetry in the synthesis of the complementary strands. The well-characterized short-chained self-replicating variants (Mills et al., 1973, 1975; Schaffner et al., 1977), however, show a remarkable symmetry in synthesis of the complementary strands. Asymmetric synthesis was detected by electrophoretic separation of double- and single-stranded RNA after extensive self-annealing by Kacian et al. (1972), who reported that MDV-1 replication produces plus strand in about 10% excess over minus strand. When analyzing the asymmetry of many of our variants (Biebricher et al., 1981a, 1982) by this common method, we always found nearly exclusively double-stranded RNA. However, in light of the kinetic theory we presented above, such results do not necessarily provide information about plus–minus asymmetries. Equal synthesis of both strands is rather expected since all known variants do form double strands and thus accumulate only double-stranded RNA in the late linear phase.

We therefore used two methods that are not masked by combination of the complementary strands. (1) We determined $[I_0^+]$, $[I_0^-]$, $[E_c^+]$, and $[E_c^-]$ for MNV-11 and MDV-1. In both the late exponential and late linear growth phases, we found ratios of $[I_0^+]/[I_0^-] = 1$ within experimental error, but the ratio $[E_c^+]/[E_c^-]$ measured in the linear growth phase was found to be 1.25 for MDV-1 and 0.8 for MNV-11, suggesting that the k_2's are different in these variants for the plus and minus strands. (2) Relaxation to the steady state after introduction of an artificial asymmetry also provides information

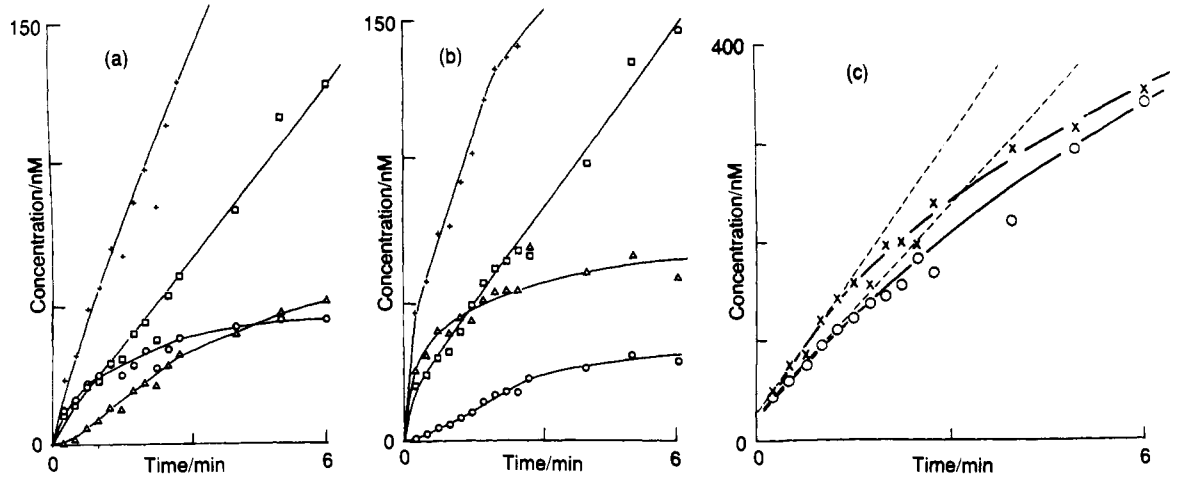

FIGURE 7: Incorporation profiles showing plus–minus asymmetry. For (a) and (b), the double-strand and the plus and minus strand bands of the gels shown in Figure 6 were cut out and counted: (a) minus strand as template; (b) plus strand as template. (+) total incorporation (sum of the bands); (○) radioactivity found in double strand; (□) radioactivity found in plus strand; (△) radioactivity found in minus strand. For (c), 5 μL of the mixtures described above was withdrawn, precipitated with 5% TCA, filtered, and counted: (×) plus strand as template; (○) minus strand as template.

about asymmetric synthesis. Starting with equimolar amounts of enzyme and plus or minus RNA strands and measuring the synthesis profiles of the two RNA strands gave the results shown in Figures 6 and 7. Synthesis starts at a much higher initial nucleotide incorporation rate since the rate-limiting reactivation of enzyme is not required before completion of one replication round. Uncompleted strands are not found among the products, indicating that elongation proceeds so rapidly that it does not influence the overall incorporation rate. In the first few minutes, only the complementary strand and double strand are produced. The occurrence of double strand is surprising. It cannot be excluded that replication may sometimes lead to the double strand; however, we consider it more likely that double strand is also produced from the intermediate IEP_n, which probably collapses to the double strand if the enzyme is removed by deproteination. On the other hand, the bands of single strands do not represent $[I^+]$ and $[I^-]$ but rather $[I^+] + [E_c^+]$ and $[I^-] + [E_c^-]$. Since the sum of both approximately equals $[E_0]$, we conclude that the free strands are the minor constituents of both sums. Incorporation with plus strand as template was reproducibly found to proceed more rapidly than that with minus strand. Since both elongation and termination are excluded as the source of this asymmetry, the latter must be caused by asymmetry in initiation. Unfortunately, the free-strand concentrations are quite small and thus difficult to measure. We would expect an excess of $[I^-]$ over $[I^+]$ if template binding rates are the reason for the asymmetry. If they were the same, differences in the geminal association step would be responsible for the rate difference. The single strands rapidly level off to unequal values, confirming the results obtained by analysis of the $[E_c^+]/[E_c^-]$ ratios. Both are thus due to the asymmetry in the reactivation rate. The observed asymmetries, however, are less than a factor of 2.

After incubation for 6 min, only the double-strand concentration increases, with an approximately linear rate. Thus, the composition of nucleic acids synthesized after several replication rounds must consist of nearly equal amounts of plus and minus strands. The results shown in Figure 7 confirm the report of Dobkin et al. (1979) on MDV-1 that enzyme is recycled in the linear growth phase via dissociation from replica and template.

Although we did not investigate the asymmetry in detail with a large number of different self-replicating RNA species, we believe that this asymmetry behavior is probably representative for short-chain self-replicating RNA species, which all have high rates of double-strand formation. With long-chain species having considerably smaller double-strand formation rates, $[I_0^+]/[I_0^-]$ ratios much different from unity may be found.

Discussion

This paper reports the extension of our previous study to an explicit distinction of plus and minus strands and the effects caused by the complementary nature of single-strand replication. The distinction is expressed as differences in the rate parameters of the two strands. The complementarity is expressed directly as double-strand formation and indirectly in the structure of the replication cycles.

The theoretical analysis shows that plus–minus asymmetries are reflected in both the exponential and linear growth phases as geometric means of certain decisive rate constants. There are notable differences between the two phases, however, and the decisive rate parameters are different for the two phases. In the exponential phase, it is the overall rate of each cycle that is rated. In the linear phase, the template binding rates alone are decisive. This difference is particularly important if selection processes in the two phases are compared, as will be shown in a subsequent paper.

Formation of double strand influences not only the quantitative outcome of replication but also the qualitative rate behavior, owing to its second-order nature. The main effect is limiting the concentrations of single strands, i.e., the strands active as template. Once the single-strand concentrations have reached their limiting values, all further material produced accumulates in the inactive double-strand form. This effect may mask the results of standard procedures for determining plus–minus asymmetries.

The results presented in this paper show how double-strand formation enters as a contribution to the rate behavior of RNA replication. Experimental analysis confirms that small plus–minus asymmetries usually do exist for short-chain, self-replicating RNA molecules.

Appendices

(I) Rate Equations for Simplified Reaction Mechanisms (Figure 1). The rate equations for E, E_c^+, and E_c^- are in both cases

$$d[E]/dt = -k_1^+[I^+][E] - k_1^-[I^-][E] + k_2^+[E_c^+] + k_2^-[E_c^-]$$

$$d[E_c^+]/dt = k_1^+[I^+][E] - k_2^+[E_c^+]$$

$$d[E_c^-]/dt = k_1^-[I^-][E] - k_2^-[E_c^-]$$

The rate equations for I^+ and I^- depend upon assumptions made about replica release and double-strand formation. If double-strand formation is neglected and replica release occurs in the first step (Figure 1a)

$$d[I^+]/dt = k_1^-[I^-][E] + k_2^+[E_c^+] - k_1^+[I^+][E]$$

$$d[I^-]/dt = k_1^+[I^+][E] + k_2^-[E_c^-] - k_1^-[I^-][E]$$

while if replica release occurs in the second step (Figure 1b)

$$d[I^+]/dt = k_2^-[E_c^-] + k_2^+[E_c^+] - k_1^+[I^+][E]$$

$$d[I^-]/dt = k_2^+[E_c^+] + k_2^-[E_c^-] - k_1^-[I^-][E]$$

If formation of double strands I^+:I^- occurs

$$d[I^+{:}I^-]/dt = k_{ds}[I^+][I^-]$$

and the term $k_{ds}[I^+][I^-]$ has to be subtracted from each of the rate equations for I^+ and I^-.

(II) Simplified Replication Mechanism in Linear Growth Phase.

Definitions:

$$[E_0] = [E_c^+] + [E_c^-] \qquad ([E] \ll [E_c^+] \text{ and } [E_c^-])$$

$$[I_0] = [I^+] + [I^-] + [E_0]$$

$$\alpha = k_1^+/k_1^- \qquad \delta = k_2^+/k_2^-$$

Reaction rates:

$$d[I^+]/dt = k_2^-[E_0]/(1 + \alpha^{1/2}/\delta)$$

$$d[I^-]/dt = k_2^+[E_0]/(1 + \delta/\alpha^{1/2})$$

$$d[I_0]/dt = k_2^+[E_0](1 + \alpha^{1/2})/(\delta + \alpha^{1/2})$$

Replication time constant:

$$\tau = \frac{\delta + \alpha^{1/2}}{k_2^+(1 + \alpha^{1/2})}$$

Concentration ratios:

$$\frac{[I^+]}{[I^-]} = \frac{1}{\alpha^{1/2}} \qquad \frac{[E_c^+]}{[E_c^-]} = \frac{\alpha^{1/2}}{\delta} \qquad \frac{[E_c^+]}{[E_0]} = \frac{1}{1 + \delta/\alpha^{1/2}}$$

$$\frac{[E_c^-]}{[E_0]} = \frac{1}{1 + \alpha^{1/2}/\delta}$$

$$\frac{[E]}{[E_0]} = \frac{k_2^+}{k_1^+} \frac{1 + \alpha^{1/2}}{1 + \delta/\alpha^{1/2}} \frac{1}{[I^+] + [I^-]}$$

These equations apply to both the consecutive (Figure 1a) and the concurrent (Figure 1b) release cases.

(III) Complete Replication Mechanism in Linear Growth Phase. For nomenclature and explanations, see Figures 4 and 5 of Biebricher et al. (1983).

Definitions:

$$k^*_{TB}{}^+ = \frac{k^*_{S1}k_{A3'}{}^+}{k_{D3'}{}^+ + k^*_{S1}{}^+}$$

Concentration ratios as in (II) with substitutions:

$$k_1^\pm \rightarrow k^*_{TB}{}^\pm \qquad k_2^\pm \rightarrow v^\pm/[E_c^\pm]$$

General rate expressions, corresponding to (II):

$$\frac{d[I^+]}{dt} = \frac{(k^*_{TB}{}^-)^{1/2}v^+v^-}{(k^*_{TB}{}^-)^{1/2}v^+ + (k^*_{TB}{}^+)^{1/2}v^-}$$

$$\frac{d[I^-]}{dt} = \frac{(k^*_{TB}{}^+)^{1/2}v^+v^-}{(k^*_{TB}{}^-)^{1/2}v^+ + (k^*_{TB}{}^+)^{1/2}v^-}$$

$$\frac{d[I_0]}{dt} = \frac{v^+v^-[(k^*_{TB}{}^+)^{1/2} + (k^*_{TB}{}^-)^{1/2}]}{(k^*_{TB}{}^-)^{1/2}v^+ + (k^*_{TB}{}^+)^{1/2}v^-}$$

Symmetric template binding:

$$k^*_{TB}{}^+ = k^*_{TB}{}^-$$

$$\frac{d[I^+]}{dt} = \frac{d[I^-]}{dt} = \frac{v^+v^-}{v^+ + v^-}$$

Symmetric rates:

$$v^+ = v^- = v \qquad d[I_0]/dt = v$$

$$\frac{d[I^+]}{dt} = \frac{v(k^*_{TB}{}^-)^{1/2}}{(k^*_{TB}{}^-)^{1/2} + (k^*_{TB}{}^+)^{1/2}}$$

$$\frac{d[I^-]}{dt} = \frac{v(k^*_{TB}{}^+)^{1/2}}{(k^*_{TB}{}^-)^{1/2} + (k^*_{TB}{}^+)^{1/2}}$$

(IV) Simplified Replication Mechanism at Steady State Caused by Double-Strand Formation.

Definitions:

$$R = d[I^+{:}I^-]/dt = k_{ds}[I^+][I^-]$$

$$\alpha = k_1^+/k_1^- \qquad \delta = k_2^+/k_2^-$$

Equations for $[E_0] = [E_c^+] + [E_c^-] + [E]$:

$$[E] = \frac{k_{ds}k_2^+}{2k_1^+k_1^-(1 + \delta)} \times \left[\left(\frac{4k_1^+k_1^-[E_0](1 + \delta)}{k_{ds}k_2^+} + 1\right)^{1/2} - 1\right]$$

$$R = \frac{k_1^+k_1^-[E]^2}{k_{ds}}$$

$$[E_c^+] = \frac{k_1^+k_1^-[E]^2}{k_2^+k_{ds}} \qquad [E_c^-] = \frac{k_1^+k_1^-[E]^2}{k_2^-k_{ds}}$$

$$[I^+] = \frac{k_1^-[E]}{k_{ds}} \qquad [I^-] = \frac{k_1^+[E]}{k_{ds}}$$

$$\frac{[I^+]}{[I^-]} = \frac{1}{\alpha} \qquad \frac{[E_c^+]}{[E_c^-]} = \frac{1}{\delta}$$

Simplified equations for $[E] \ll [E_0]$:

$$R = \frac{k_2^+[E_0]}{1 + \delta} \qquad [E] = \left(\frac{[E_0]k_{ds}k_2^+}{k_1^+k_1^-(1 + \delta)}\right)^{1/2}$$

$$\frac{[E_c^+]}{[E_0]} = \frac{1}{1 + \delta} \qquad \frac{[E_c^-]}{[E_0]} = \frac{1}{1 + 1/\delta}$$

These equations apply to both the consecutive (Figure 1a) and the concurrent (Figure 1b) release cases.

(V) Simplified Replication Mechanisms in Exponential Growth Phase. After an induction period, all concentrations grow in constant ratios such that they obey

$$\frac{1}{[X]}\frac{d[X]}{dt} = \frac{d \ln [X]}{dt} = \kappa$$

(*a*) *Concurrent Release* (*Figure 1b*). Substituting $\kappa[X]$ for the left-hand sides of the rate equations for I^+, I^-, E_c^+, and E_c^- pertaining to replica release in step 2 (Appendix I) and introducing the sums $[I_0^+] = [I^+] + [E_c^+]$ and $[I_0^-] = [I^-] + [E_c^-]$ leads to the quartic equation for the first two cases of one-step self-replication:

$$[\kappa^2 + \kappa(k_1^+[E_0] + k_2^+)][\kappa^2 + \kappa(k_1^-[E_0] + k_2^-)] = k_1^+k_1^-[E_0]^2k_2^+k_2^-$$

If step 1 is rate limiting, the conditions $k_2^+ \gg k_1^+[E_0]$ and $k_2^- \gg k_1^-[E_0]$ hold, and it reduces to

$$(\kappa^2 + \kappa k_2^+)(\kappa^2 + \kappa k_2^-) = k_1^+k_1^-[E_0]^2k_2^+k_2^-$$

Since $\kappa \ll k_2^+$ and k_2^-, a geometric mean growth constant is obtained:

$$\kappa = (k_1^+k_1^-)^{1/2}[E_0]$$

If step 2 is rate limiting, the converse conditions $k_2^+ \ll k_1^+[E_0]$ and $k_2^- \ll k_1^-[E_0]$ pertain, and the quartic equation reduces to

$$(\kappa^2 + \kappa k_1^+[E_0])(\kappa^2 + \kappa k_1^-[E_0]) = k_1^+k_1^-[E_0]^2k_2^+k_2^-$$

Since $\kappa \ll k_1^+[E_0]$ and $k_1^-[E_0]$, the alternative geometric mean growth constant

$$\kappa = (k_2^+k_2^-)^{1/2}$$

is obtained.

(*b*) *Consecutive Release* (*Figure 1a*). If the rate equations pertaining to replica release in step 1 are used, the different quartic equation

$$\kappa^2[\kappa^2 + \kappa(k_1^+[E_0] + k_1^-[E_0] + k_2^+ + k_2^-) + (k_1^+[E_0] + k_2^+)(k_1^-[E_0] + k_2^-)] = k_1^+k_1^-[E_0]^2[\kappa^2 + \kappa(k_2^+ + k_2^-) + k_2^+k_2^-]$$

is obtained. If step 1 is rate limiting, $k_2^+ \gg k_1^+[E_0]$ and $k_2^- \gg k_1^-[E_0]$, giving the third case of one-step self-replication. The two bracketed groups become equal, and the polynomial reduces to $\kappa^2 = k_1^+k_1^-[E_0]^2$, which yields the same geometric mean growth constant as above:

$$\kappa = (k_1^+k_1^-)^{1/2}[E_0]$$

If step 2 is rate limiting, the converse conditions $k_2^+ \ll k_1^+[E_0]$ and $k_2^- \ll k_1^-[E_0]$ pertain, and two-step self-replication occurs. The inequalities $k_2^+ \ll \kappa \ll k_1^+[E_0]$ and $k_2^- \ll \kappa \ll k_1^-[E_0]$ hold, yielding for the growth constant a different result:

$$\kappa = [k_1^+k_1^-[E_0](k_2^+ + k_2^-)/(k_1^+ + k_1^-)]^{1/2}$$

The dependence on $[E_0]$ in the above equations disappears for enzyme saturation conditions when step 1 no longer refers to the template binding process (see text).

(*VI*) *Concentration Ratios in Exponential Growth Phase.* The derivatives of $[E_c^+]$ and $[E_c^-]$ (Appendix V) are $\kappa[E_c^+]$ and $\kappa[E_c^-]$, respectively, during the exponential growth phase. Setting $[E]$ equal to $[E_0]$ and solving these equations gives the ratios of free and bound RNA:

$$\frac{[I^+]}{[E_c^+]} = \frac{\kappa + k_2^+}{k_1^+[E_0]} \qquad \frac{[I^-]}{[E_c^-]} = \frac{\kappa + k_2^-}{k_1^-[E_0]}$$

The plus to minus ratios depend upon whether replica release occurs concurrently or consecutively. Setting the derivatives of $[I^+]$ and $[I^-]$ equal to $\kappa[I^+]$ and $\kappa[I^-]$, respectively, leads, with the above equations, to the following formulas.

(*a*) *Consecutive Release* (*Figure 1a*).

$$\frac{[I^+]}{[I^-]} = \kappa\frac{k_1^-}{k_1^+}\left(\frac{1}{k_1^-[E_0]} + \frac{1}{\kappa + k_2^-}\right)$$

$$\frac{[I_0^+]}{[I_0^-]} = \frac{\kappa(\kappa + k_2^+ + k_1^+[E_0])}{k_1^+[E_0](\kappa + k_2^+)}$$

These formulas may be simplified in accordance with the limiting formulas for the growth constant κ given in Appendix V. If step 1 is rate limiting, $k_1[E_0] \ll \kappa \ll k_2$ holds, and the above formulas become

$$\frac{[I^+]}{[I^-]} \to \left(\frac{k_1^-}{k_1^+}\right)^{1/2} \qquad \frac{[I_0^+]}{[I_0^-]} \to \frac{k_1^-}{k_1^+}$$

If step 2 is rate limiting, $k_1[E_0] \gg \kappa \gg k_2$ holds, and the limiting formulas are

$$\frac{[I^+]}{[I^-]} \to \frac{k_1^-}{k_1^+} \qquad \frac{[I_0^+]}{[I_0^-]} \to 1$$

(*b*) *Concurrent Release* (*Figure 1b*).

$$\frac{[I^+]}{[I^-]} = \frac{\kappa + k_1^-[E_0]}{\kappa + k_1^+[E_0]}$$

$$\frac{[I_0^+]}{[I_0^-]} = \frac{\kappa(\kappa + k_2^+ + k_1^+[E_0])}{k_2^+k_1^+[E_0]}$$

If step 1 is rate limiting

$$\frac{[I^+]}{[I^-]} \to 1 \qquad \frac{[I_0^+]}{[I_0^-]} \to \left(\frac{k_1^-}{k_1^+}\right)^{1/2}$$

If step 2 is rate limiting

$$\frac{[I^+]}{[I^-]} \to 1 \qquad \frac{[I_0^+]}{[I_0^-]} \to \left(\frac{k_1^-}{k_1^+}\right)^{1/2}$$

The dependence on $[E_0]$ in the above equations disappears for enzyme saturation conditions when step 1 no longer refers to the template binding process (see text).

(*VII*) *Multistep Replication Mechanism for Exponential Growth Phase.* The rate constant matrix **K** for the mechanism of Figure 4 is

$$\begin{pmatrix}
-\mathbf{k}_1^+ & 0 & \cdots & 0 & +\mathbf{k}_n^+ & 0 & \cdots & 0 & +\mathbf{k}_n^- \\
+\mathbf{k}_1^+ & -\mathbf{k}_2^+ & & & & & & & 0 \\
0 & +\mathbf{k}_2^+ & -\mathbf{k}_3^+ & & & & & & \vdots \\
\vdots & \ddots & \ddots & & & & & & \vdots \\
 & & & & & & & & \\
 & & & & +\mathbf{k}_{n-1}^+ & -\mathbf{k}_n^+ & & & 0 \\
 & & & & & +\mathbf{k}_n^+ & -\mathbf{k}_1^- & & +\mathbf{k}_n^- \\
 & & & & & & +\mathbf{k}_1^- & -\mathbf{k}_2^- & 0 \\
 & & & & & & & \ddots & \vdots \\
 & & & & & & & & \vdots \\
 & & & & & & & & \vdots \\
 & & & & & & & & \vdots \\
 & & & & & & & & 0 \\
0 & \cdots & & & & & & 0 & +\mathbf{k}_{n-1}^- - \mathbf{k}_n^-
\end{pmatrix}$$

For equal rate constants at each step, i.e., $k_i^+ = k^+$ and k_i^-

$= k^-$, it has the characteristic equation

$$(k^+ + \lambda)[(k^- + \lambda)^n - (k^-)^n] - (k^+)^n[(k^- + \lambda)^n - (k^-)^n] - (k^+)^n(k^-)^n = 0$$

which can be reduced to

$$(1 + \lambda/k^+)^{-n} + (1 + \lambda/k^-)^{-n} = 1$$

and solved implicitly for λ/k^+ for assumed values of n and k^+/k^-. For large values of n, λ/k^+ and λ/k^- become very small, and the characteristic equation can be written in exponential notation:

$$\exp(-n\lambda/k^+) + \exp(-n\lambda/k^-) = 1$$

which can be solved for assumed values of k^+/k^-, e.g.

$$k^+/k^- = 1 \qquad \lambda/k^+ = (1/n) \ln 2$$

$$k^+/k^- = 2 \text{ or } \tfrac{1}{2} \qquad \lambda/k^+ = (1/n) \ln [2/(5^{1/2} - 1)]$$

Registry No. Qβ replicase, 9026-28-2.

References

Biebricher, C. K. (1983) in *Evolutionary Biology* (Hecht, M. K., Wallace, B., & Prance, G. T., Eds.) Vol. 16, pp 1-52, Plenum Press, New York.

Biebricher, C. K., Eigen, M., & Luce, R. (1981a) *J. Mol. Biol. 148*, 369-390.

Biebricher, C. K., Eigen, M., & Luce, R. (1981b) *J. Mol. Biol. 148*, 391-410.

Biebricher, C. K., Diekmann, S., & Luce, R. (1982) *J. Mol. Biol. 154*, 629-648.

Biebricher, C. K., Eigen, M., & Gardiner, W. C., Jr. (1983) *Biochemistry 22*, 2544-2559.

Dobkin, C., Mills, D. R., Kramer, F. R., & Spiegelman, S. (1979) *Biochemistry 18*, 2038-2044.

Eigen, M. (1971) *Naturwissenschaften 58*, 465-523.

Feix, G., Pollet, R., & Weissmann, C. (1968) *Proc. Natl. Acad. Sci. U.S.A. 59*, 145-152.

Kacian, D. L., Mills, D. R., Kramer, F. R., & Spiegelman, S. (1972) *Proc. Natl. Acad. Sci. U.S.A. 69*, 3038-3042.

Mills, D. R., Peterson, R. L., & Spiegelman, S. (1967) *Proc. Natl. Acad. Sci. U.S.A. 58*, 217-224.

Mills, D. R., Kramer, F. R., & Spiegelman, S. (1973) *Science (Washington, D.C.) 180*, 916-927.

Mills, D. R., Kramer, F. R., Dobkin, C., Nishihara, T., & Spiegelman, S. (1975) *Proc. Natl. Acad. Sci. U.S.A. 72*, 4252-4256.

Mills, D. R., Dobkin, C., & Kramer, F. R. (1978) *Cell (Cambridge, Mass.) 15*, 541-550.

Nishihara, T., Mills, D. R., & Kramer, F. R. (1983) *J. Biochem. (Tokyo) 93*, 669-674.

Prives, L. C., & Silverman, P. (1972) *J. Mol. Biol. 71*, 657-670.

Schaffner, W., Rüegg, K. J., & Weissmann, C. (1977) *J. Mol. Biol. 117*, 877-907.

Silverman, P. M. (1973) *Arch. Biochem. Biophys. 157*, 234-242.

Formation and Rejoining of Deoxyribonucleic Acid Double-Strand Breaks Induced in Isolated Cell Nuclei by Antineoplastic Intercalating Agents†

Yves Pommier,* Ronald E. Schwartz, Kurt W. Kohn, and Leonard A. Zwelling

ABSTRACT: The biochemical characteristics of the formation and disappearance of intercalator-induced DNA double-strand breaks (DSB) were studied in nuclei from mouse leukemia L1210 cells by using filter elution methodology [Bradley, M. O., & Kohn, K. W. (1979) *Nucleic Acids Res. 7*, 793-804]. The three intercalators used were 4′-(9-acridinylamino)-methanesulfon-*m*-anisidide (*m*-AMSA), 5-iminodaunorubicin (5-ID), and ellipticine. These compounds differ in that they produced predominantly DNA single-strand breaks (SSB) (*m*-AMSA) or predominantly DNA double-strand breaks (ellipticine) or a mixture of both SSB and DSB (5-ID) in whole cells. In isolated nuclei, each intercalator produced DSB at a frequency comparable to that which is produced in whole cells. Moreover, these DNA breaks reversed within 30 min after drug removal. It thus appeared that neither ATP nor other nucleotides were necessary for intercalator-dependent DNA nicking–closing reactions. The formation of the intercalator-induced DSB was reduced at ice temperature. Break formation was also reduced in the absence of magnesium, at a pH above 6.4 and at NaCl concentrations above 200 mM. In the presence of ATP and ATP analogues, the intercalator-induced cleavage was enhanced. These results suggest that the intercalator-induced DSB are enzymatically mediated and that the enzymes involved in these reactions can catalyze DNA double-strand cleavage and rejoining in the absence of ATP, although the occupancy of an ATP binding site might convert the enzyme to a form more reactive to intercalators. Three inhibitors of DNA topoisomerase II—novobiocin, nalidixic acid, and norfloxacin—reduced the formation of DNA strand breaks. These findings are consistent with the hypothesis that intercalator-induced DNA breakage results from the DNA cleavage action of a DNA topoisomerase II.

DNA intercalators produce strand breaks in cellular DNA (Ross et al., 1978; Zwelling et al., 1981, 1982a,d). The formation of these breaks tends toward saturation at high drug concentration and is temperature dependent (Zwelling et al., 1981, 1982d). The DNA breaking activity, with biochemical properties similar to those of intercalator-induced DNA scission, can be reconstituted in a cell-free system by means of a 0.35 M NaCl extract of isolated nuclei (Filipski et al., 1983). These characteristics have suggested that the formation of intercalator-induced DNA breaks is mediated by enzymes associated with chromatin. In addition, several aspects of this intercalator-induced DNA breakage have suggested that the

† From the Laboratory of Molecular Pharmacology, Developmental Therapeutics Program, Division of Cancer Treatment, National Cancer Institute, National Institutes of Health, Bethesda, Maryland 20205. *Received August 30, 1983; revised manuscript received January 23, 1984.*